

# **CNWRA** A center of excellence in earth sciences and engineering

A Division of Southwest Research Institute™  
6220 Culebra Road • San Antonio, Texas, U.S.A. 78228-5166  
(210) 522-5160 • Fax (210) 522-5155

February 13, 2001  
Contract No. NRC-02-97-009  
Account No. 20.01402.671

U.S. Nuclear Regulatory Commission  
ATTN: Mrs. Deborah A. DeMarco  
Two White Flint North  
11545 Rockville Pike  
Mail Stop T8 A23  
Washington, DC 20555

Subject: Programmatic Review of a Paper

Dear Mrs. DeMarco:

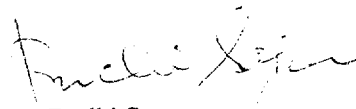
The enclosed paper, which will be submitted for presentation at the 38<sup>th</sup> U.S. Rock Mechanics Symposium to be held in Washington, DC on July 7–10th, 2001 is being submitted for programmatic review. The title of the paper is:

“Hydrological Implications of Thermally Induced Geomechanical Response at Yucca Mountain, Nevada”  
by Goodluck Ofoegbu

This paper is based on the report Thermal-Mechanical Effects on Long-Term Hydrological Properties at the Proposed Yucca Mountain Nuclear Waste Repository, which was submitted to NRC on June 22, 2000, in fulfillment of Milestone No. 20.01402.671.040 and was accepted by NRC on July 27, 2000. This paper presents a summary of the report’s main conclusions that significant changes in long-term hydrological properties owing to thermally induced geomechanical response can be expected and that such changes would result in a redistribution of moisture flux at the repository level. An extended abstract of the paper was submitted to NRC on September 29, 2000 and was accepted by NRC on October 6, 2000.

Please advise me of the results of your programmatic review. Your cooperation in this matter is appreciated.

Sincerely,



Budhi Sagar  
Technical Director

cc:	J. Linehan	T. Essig	M. Nataraja	CNWRA EMs
	W. Reamer	S. Wastler	B. Jagannath	G.I. Ofoegbu
	B. Meehan	D. Brooks	W. Patrick	A. Ghosh
	G. Greeves	N.K. Stablein	CNWRA Dirs	S. Hsiung



Washington Office • Twinbrook Metro Plaza #210  
12300 Twinbrook Parkway • Rockville, Maryland 20852-1606

# Hydrological Implications of Thermally Induced Geomechanical Response at Yucca Mountain, Nevada

Goodluck I Ofoegbu

Center for Nuclear Waste Regulatory Analyses, Southwest Research Institute

**ABSTRACT:** Geomechanical response to thermal loading at the proposed Yucca Mountain repository for high-level nuclear waste may result in changes in rock-mass hydrological properties within laterally discontinuous zones in the repository horizon. The altered zones would be characterized by increased horizontal permeability and their development will depend on the thermal loading, rock-mass thermal and mechanical properties, and design features such as ventilation that may affect heat transfer into the host rock. Lateral diversion of moisture within or around the altered zones can be expected and would result in a redistribution of the cross-repository moisture flux. Lateral flow would be directed down-dip of the site-scale stratigraphy. Therefore, cross-repository moisture flux would be reduced at the up-dip ends of the thermal-mechanical altered zones and increased at the down-dip ends. Consequently, parts of an emplacement drift close to the down-dip end of a thermal-mechanical altered zone can be expected to experience elevated percolation flux.

## 1 INTRODUCTION

The host rock mass for the proposed repository at Yucca Mountain may undergo changes in hydrological properties owing to the geomechanical response of the rock mass to the heat generated by radioactive decay of nuclear waste. Changes in hydrological properties should be considered because of their potential effect on the amounts of water seepage (percolation flux) through the repository horizon. An understanding of the temporal and spatial distributions of percolation flux is essential to predict the occurrence and magnitudes of seepage into the emplacement drifts, and, therefore, the onset and rates of waste-package corrosion and the transport of radionuclides in aqueous states to the saturated zone.

Thermally induced geomechanical response (in addition to responses induced by excavation and potential seismic loading) may induce changes in fracture aperture and, hence, fracture porosity, permeability, and, possibly, capillarity. Thermal-mechanical response will be controlled by the geometry of the emplacement area, thermal and mechanical properties of the rock mass, nature and distribution of waste packages, and other design features (such as ventilation) that may affect heat transfer from the waste packages to the rock mass. The emplacement geometry [Civilian Radioactive

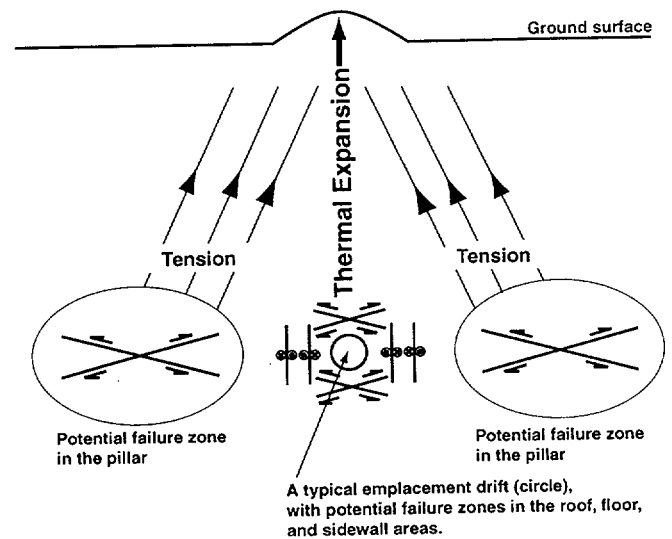


Figure 1. Schematic illustration of the anticipated mechanisms of thermal-mechanical response, showing the effects of emplacement geometry on the distributions of zones of potential rock failure in a horizontal array of drifts. Actual development of the failure zones would be determined by the induced temperature and rock-mass mechanical properties.

Waste Management System (2000)] consists of a horizontal array of drifts at a depth of about 300 m below the ground surface. For a typical drift within the array, thermal expansion of the surrounding rock would be fully suppressed laterally but a limited amount of vertically upward expansion can occur because of free movement at the ground surface (Figure 1).

Consequently, the anticipated horizontal component of thermal stress is much higher than the vertical component, except close to the sidewall of the drift openings where the vertical component of thermal stress would be higher than the drift-normal horizontal component because of the closeness of a traction-free boundary. The upward expansion of the heated zones around a drift would impose an upward pull on cooler areas in the pillars, resulting in thermally induced tension in the vertical direction (figure 1). The vertical component of rock stress near the pillar centers would, thus, be expected to decrease and may occasionally be tensile. These stress conditions, which depend only on the emplacement geometry, favor the development of potential zones of rock failure (by fracture slip) following the mechanisms illustrated in Figure 1, i.e., reverse-faulting style in the roof and floor areas of the drifts and in the pillars, and strike-slip or normal-faulting styles near the drift sidewalls.

The magnitudes of the induced stresses and whether such stresses are sufficient to cause rock failure depend on the induced temperature and the rock-mass mechanical properties. The magnitude of induced stress caused by a given change in temperature is determined by the rock-mass thermal expansivity,  $\alpha$ , and the Young's modulus,  $E$ , whereas the rock-mass strength determines whether the induced stress is sufficient to cause failure. The effects of these material properties on the anticipated thermal-mechanical response and the hydrological implications of such response are examined in this paper. Changes in fracture aperture owing to repository thermal loading were determined from a series of analyses based on a drift-scale finite element model, and the effects of the aperture changes on repository-level percolation flux were examined using a site-scale thermal-hydrological model.

## 2 THERMAL-MECHANICAL MODEL

Thermal-mechanical analyses were performed using a two-dimensional (plane strain) model extending 40.5 m horizontally and 670 m vertically. The emplacement drift is represented in the model as a vertical semicircle of 5.5-m diameter. The model extends horizontally from the center of the drift to the middle of the adjacent pillar on one side of the drift, representing a drift center-to-center spacing of 81 m as specified in the current proposed-repository design (Civilian Radioactive Waste Management System, Management and Operating Contractor 1999); and vertically from the ground surface to the water table, with the drift axis located at a depth of 320 m below the ground surface. The thermal and mechanical properties used for the model are given in Table 1, with the justifications for the property values given in Ofoegbu (2000).

The thermal boundary conditions consist of fixed temperature at the top (ground surface) and base (water table) of the model and zero heat flux normal to the vertical boundaries. The excavated drift was not included in the thermal-analysis model. Instead, a volumetric heat source (defined in Table 1) was applied within material inside the drift perimeter. The mechanical boundary conditions are zero vertical displacement at the base, zero horizontal displacement on the vertical boundaries, and free-surface condition at the top.

Table 1. Rock-mass thermal and mechanical parameters

Parameter name	Value
Initial vertical stress	Based on vertical gradient of 0.022 MPa/m
Initial horizontal-to-vertical stress ratio	0.266 (Based on Poisson's ratio of 0.21)
Thermal loading	1.226 kW/m of drift initially, decaying to 0.0166 kW/m at 10,000 yr
Density	2,210 kg/m <sup>3</sup>
Thermal conductivity	2.13 W/m·K
Specific heat capacity (J/kg·K)	969, 4741, and 988 at temperature of <94, 94–114, and >114 °C, respectively.
Poisson's ratio	0.21
Thermal expansivity (10 <sup>-6</sup> /K)	Varies with temperature from 7.14 at 0–50 °C to 15.5 at 200 °C
Young's modulus	7.8 GPa for rock mass quality category RMQ1, and 32.6 GPa for RMQ5 category
Friction angle	27.5° for RMQ1 and 34.4° for RMQ5
Cohesion (MPa)	2.82 MPA for RMQ1 and 5.08 MPA for RMQ5

The drift opening was not included in the model at the start, but was introduced by removing materials within the drift perimeter after the initial equilibrium state (from in-situ stress) was established. The drift perimeter was treated as a free surface thereafter. The thermal and mechanical boundary conditions on the vertical boundaries simulate vertical symmetry planes. The initial temperature was defined using a temperature of 18.7 °C at the ground surface and the geothermal gradient for the site (cf. Ofoegbu, 2000), which gives a temperature of 34.3 °C at the model base

Thermal-mechanical analyses were conducted using ABAQUS Version 5.8, a commercial finite element code (Hibbit, Karlsson & Sorensen, Inc., 1998). Each analysis consists of a set of sequentially coupled heat-conduction and static stress analyses. The heat conduction analysis was performed for a simulation period of 150 yr from waste emplacement, and the resulting temperature histories were used as input for the associated static stress analyses. The stress analysis consisted of an initial step to establish the static equilibrium state prior to drift excavation, a second step during which material within the drift perimeter was removed to simulate excavation, and a third and final step during which the temperature histories from the heat conduction analysis were applied to calculate the geomechanical response to the simulated thermal loading.

Both linear-elastic and elastic-plastic analyses were performed and the values of the mechanical properties were varied as shown in Table 1 to represent two bounding rock-mass quality categories (Ofoegbu, 2000). As shown in the following sections, the linear-elastic models were found very useful in understanding the potential distributions of rock-failure susceptibility and the effects of rock-mass quality on the distributions.

### 3 STRESS HISTORIES AND FAILURE SUSCEPTIBILITY

Results from linear-elastic analyses (Figures 2, 3, and 4) indicate a general increase in compressive stress during the first 20–25 yr after waste emplacement and a general decrease in stress thereafter. The magnitudes of thermally induced stress are much higher in the

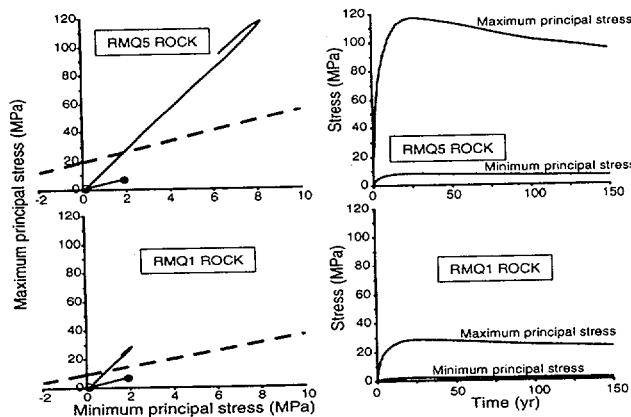


Figure 2. Stress path and histories at a point near the drift roof from linear-elastic analyses, showing the effects of Young's modulus. Dashed lines represent rock strength. The filled and open circles represent the stress states before and after excavation (prior to waste emplacement) respectively.

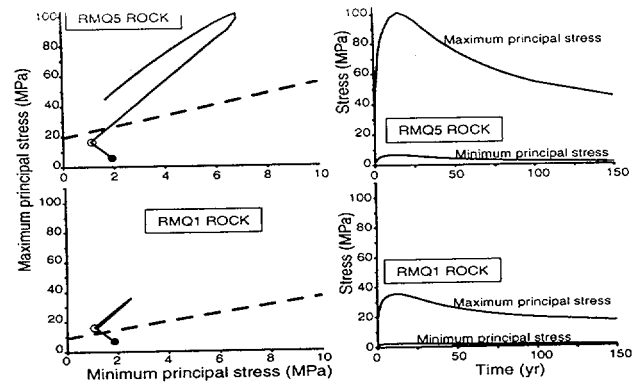


Figure 3. Stress path and histories at a point near the drift sidewall from linear-elastic analyses, showing the effects of Young's modulus. Dashed lines represent rock strength. The filled and open circles represent the stress states before and after excavation (prior to waste emplacement) respectively.

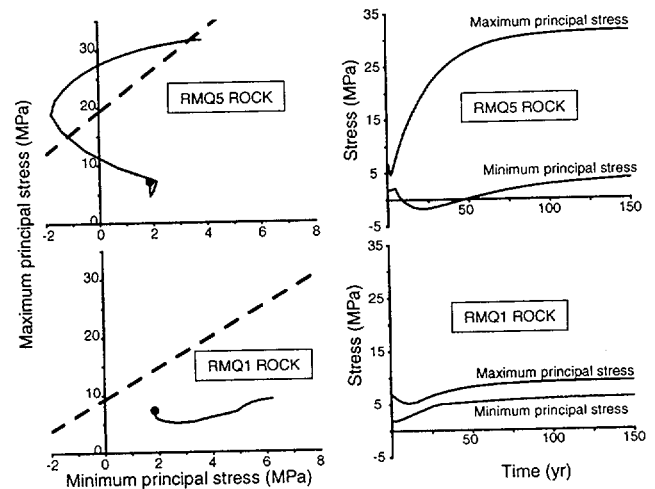


Figure 4. Stress path and histories at a point near the pillar center from linear-elastic analyses, showing the effects of Young's modulus. Dashed lines represent rock strength and the filled circle represents the initial stress state.

higher-stiffness rock (e.g., RMQ5) than in the lower-stiffness rock (e.g., RMQ1).

The roof areas of the drifts would experience a decrease in stress during excavation (indicated by the change from the filled circle to the open circle along the stress paths in Figure 2) followed by an increase in stress owing to thermal loading. Fractured rock in the roof area would, thus, become more loose during and after excavation, but the loosening would be reversed by the increase in compressive stress from thermal loading. The increased compressive stress may

subsequently cause rock failure in the roof areas as indicated by the stress paths rising above the strength surfaces (dashed lines) in Figure 2. The maximum principal stress would be horizontal, and the minimum would be vertical, in the roof area during the thermal regime. Therefore, thermally induced rock failure in the roof area would consist of slip on subhorizontal fractures, following the reverse-faulting style as indicated in Figure 1. Similar results were obtained from discontinuum-model calculations (e.g., Ofoegbu et al, 2001), which indicate thermally induced slip on subhorizontal fractures in the roof area.

The effect of excavation on the stress states in the sidewall area (indicated by the change from the filled circle to the open circle along the stress paths in Figure 3) would consist of a decrease in the minimum principal stress and an increase in the maximum principal stress, causing the stress path to rise toward the strength surface (dashed line). Both principal stresses would increase thereafter because of thermal loading, with the maximum principal stress increasing more than the minimum, giving a stress path that would approach and may ultimately intersect the strength surface. Therefore, rock failure may occur in the sidewall area both before and during the thermal regime, and would consist of slip on subvertical fractures. A similar sidewall failure mechanism, i.e., slip on subvertical fractures, was obtained from discontinuum modeling (e.g., Ofoegbu et al, 2001).

Thermal-mechanical response in the mid-pillar areas is strongly dependent on the rock-mass stiffness as shown in Figure 4. Mid-pillar areas in high-stiffness rock such as RMQ5 would experience an increase in the principal-stress difference during the thermal regime. This is in contrast with the response in mid-pillar areas located in low-stiffness rock such as RMQ1, which would experience a decrease in the principal-stress difference during the thermal regime. Consequently, thermal loading would cause the stress path in mid-pillar areas to either approach the failure surface in high-stiffness rock such as RMQ5 or move farther from the failure surface in low-stiffness rock such as RMQ1 (Figure 4). Therefore, thermal loading would increase the likelihood of failure for pillars in high-stiffness rock but decrease it for pillars in low-stiffness rock. The calculated stress directions in the mid-pillar area during the thermal regime are horizontal for the maximum principal stress and vertical for the minimum principal stress. Therefore, thermally induced rock failure would consist of slip on subhorizontal fractures, following the reverse-faulting style as indicated in Figure 1. This failure mechanism is consistent with the results from discontinuum-model calculations (e.g., Ofoegbu et al, 2001), which indicate thermally induced slip on subhorizontal fractures in the pillars in areas of high-stiffness rock.

The distribution of rock-failure susceptibility would vary with time and rock-mass stiffness as shown in Figure 5. The failure susceptibility  $F_s$  is defined as the ratio  $\sigma_{\max}/\sigma_f$ , where  $\sigma_{\max}$  is the maximum principal stress and  $\sigma_f$  is the compressive strength calculated using the Mohr-Coulomb strength criterion. Values of  $F_s \geq 1$  represent locations at which rock failure would occur (based on the model mechanical parameters). For  $F_s < 1$ , the stress states approach the failure conditions as  $F_s$  approaches 1.

The figure indicates two potential rock-failure zones: one around the drift and a second centered in the pillar. The development of the mid-pillar failure zone would be more likely in higher-stiffness rock (RMQ5) and less likely in lower-stiffness rock (RMQ1). This pattern of rock-failure distribution is consistent with the patterns obtained from other studies based on continuum modeling with elastic-plastic material behavior (Ofoegbu, 1999, 2000). The potential failure zone around the drift may impact the stability of the openings, but the potential failure zone in the pillar would not impact the stability of the openings if the associated fracture slip is localized within the pillar. Both potential failure zones would, however, impact the hydrological properties and consequently moisture flow.

#### 4 CHANGE IN HYDROLOGICAL PROPERTIES

Changes in fracture aperture owing to thermally induced geomechanical response result in changes in hydrological properties, such as fracture porosity, permeability, and capillarity. A fracture-aperture change may arise directly from a change in the fracture normal stress or from fracture-network dilation associated with fracture slip. An increase in compressive stress, such as would occur around the emplacement drifts as noted earlier, would cause a general decrease in fracture aperture. However, aperture-versus-depth data interpreted from injection tests performed at several dam sites (Snow, 1968; Wei et al., 1995) indicate that fractures located at a depth of a few tens of meters or greater are likely to have attained maximum closure (minimum aperture). An increase in compressive stress at such depth is therefore, not likely to cause an appreciable decrease in fracture aperture. For this reason, the anticipated thermally induced increase in compressive stress at such depth in the proposed emplacement area is not likely to cause any appreciable decrease in fracture aperture. On the other hand, an increase in fracture aperture is anticipated to result from excavation-induced rock loosening in the roof area and thermally induced fracture-network dilation associated with slip in the roof, floor, sidewall, and mid-pillar areas.

The distribution of the dilation zones (referred to hereafter as altered zones) would follow the pattern of

failure susceptibility in Figure 5. That is, altered zones centered at the drifts and in the middle of the pillars would be expected. Although the adjacent drift-centered and pillar-centered altered zones may

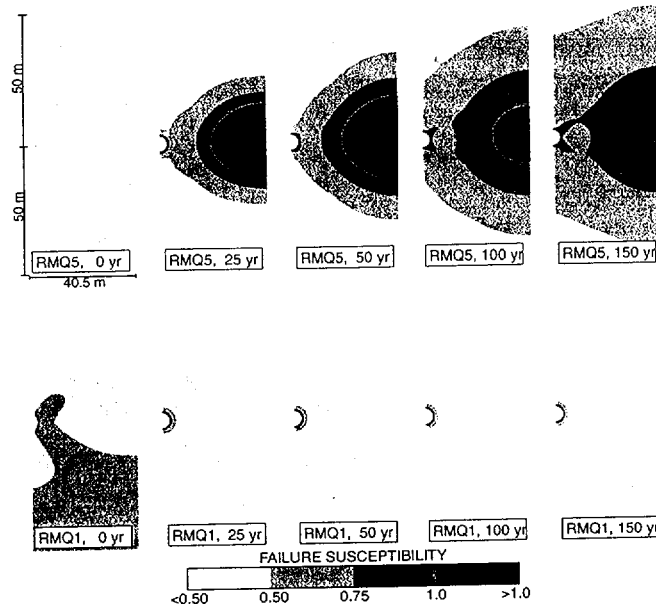


Figure 5. Distributions of rock-failure susceptibility based on stresses from linear-elastic analyses. The plots illustrate the effects of emplacement geometry and rock-mass quality (RMQ1 and RMQ5) on failure susceptibility.

coalesce, the altered zones are expected to be laterally discontinuous because of the variability of mechanical properties. The results in Figure 5, for example, suggest that an altered zone in a RMQ5 area would not extend into adjacent RMQ1 area. Because slip on subhorizontal fractures is the dominant mechanism of the anticipated thermally induced rock failure

(Figure 1), the altered zones would be characterized by increased horizontal permeability (e.g., Barton et al., 1995).

## 5 EFFECTS ON MOISTURE FLOW

A series of thermal-hydrological analyses was performed using a site-scale model (Figure 6) to examine the effects of a generic, laterally discontinuous, thermal-mechanical-altered zone on moisture flow. Analyses were performed for a net ground-surface infiltration rate of 10 mm/yr. Thermal-hydrological behavior was simulated using the mass and energy transport module of MULTIFLO, a thermal-hydrological-chemical simulation system (Lichtner et al., 2000). A detailed description of the model is given in another publication (Ofoegbu et al., 2001).

The analyses examined variations in the cross-repository moisture flux, i.e., flux crossing the thick dashed line in Figure 6. The general direction of flow is vertically downward with a small west-to-east flux component caused by the easterly dip of the site-scale stratigraphy (Ofoegbu et al., 2001). This flow pattern may be modified locally within the repository horizon owing to the development of a thermal-mechanical-altered zone (e.g., ellipse in Figure 6). Results are presented in Figure 7, for example, to illustrate the effects of a generic altered zone that may act as a conduit or a flow barrier. An altered zone in an unsaturated medium would tend to act as a flow barrier if the thermal-mechanical changes cause a reduction in the capillarity of the medium. Such capillarity changes were not modeled directly, but their potential effects

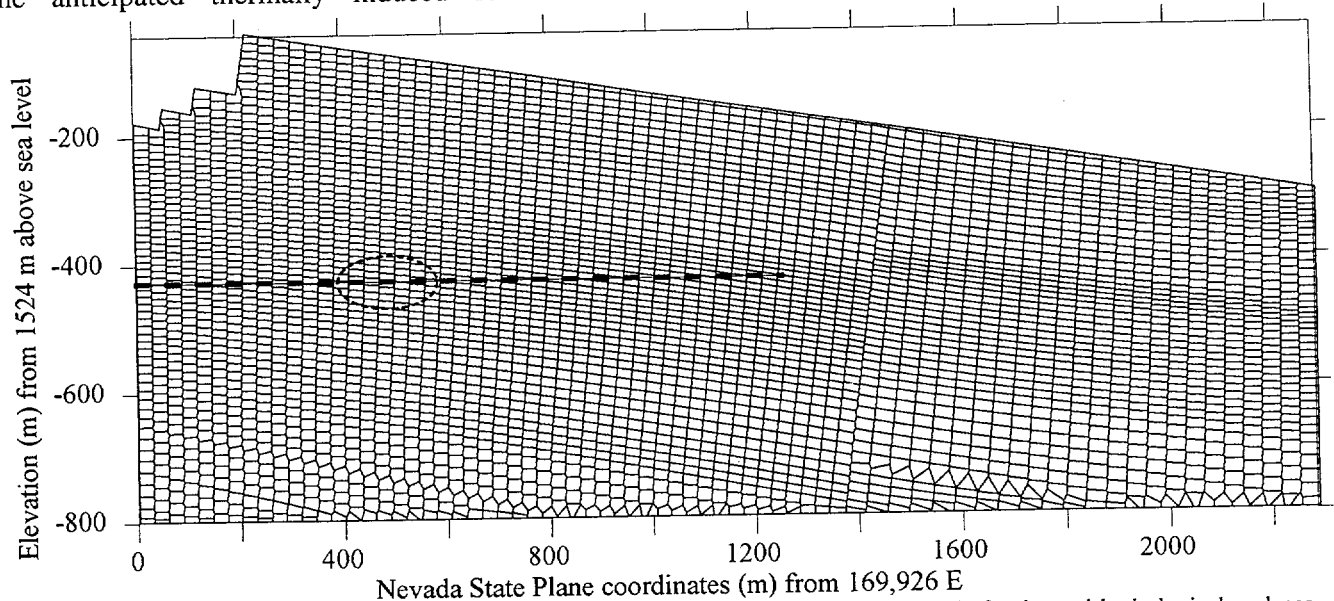


Figure 6. Finite difference discretization of an east-west vertical section through Yucca Mountain for thermal-hydrological analyses (from Ofoegbu et al., 2001). The thick horizontal dashed line represents the repository axis, and the horizontal ellipse with dashed boundary represents a generic thermal-mechanical altered zone.

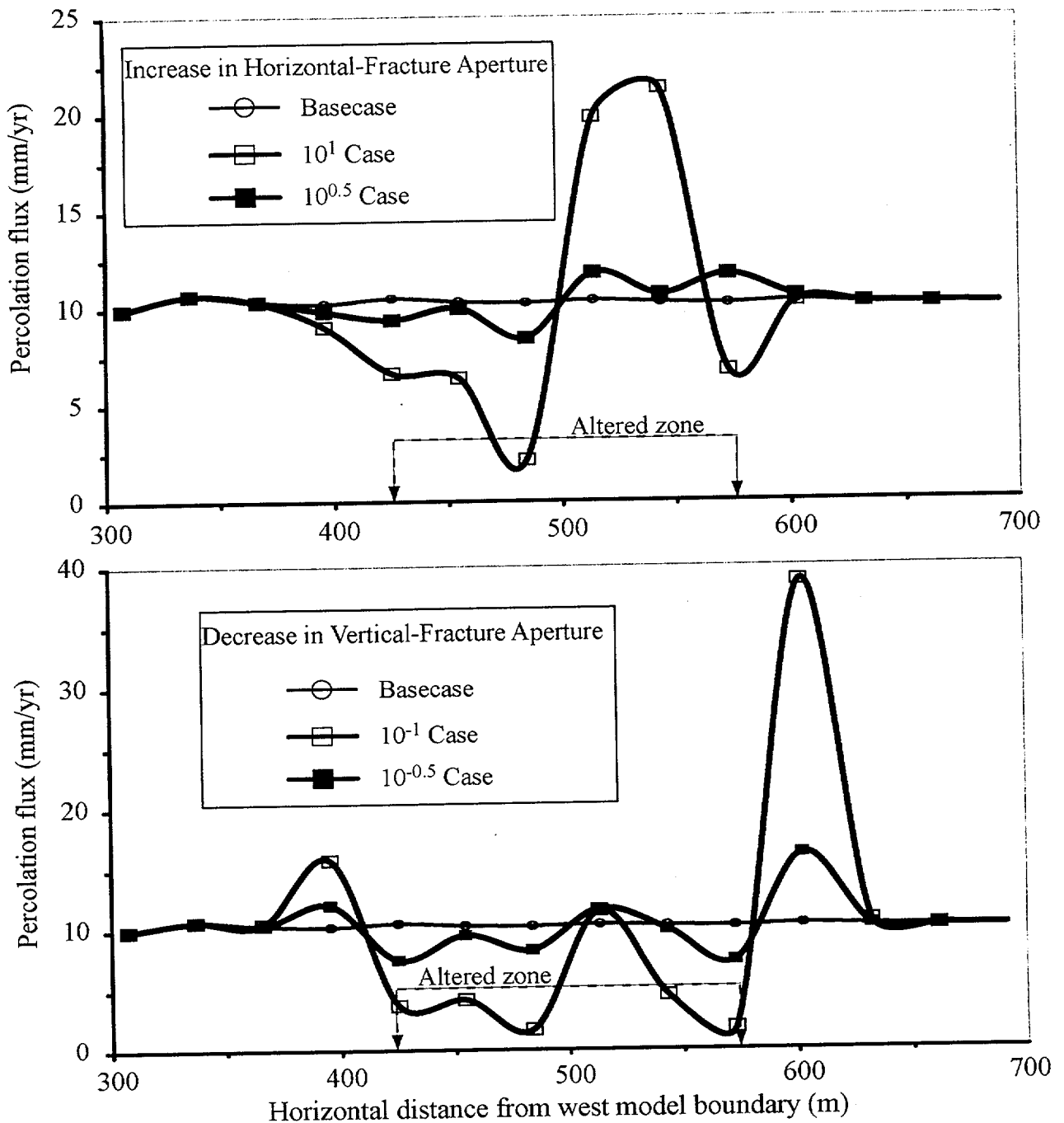


Figure 7. Profiles of cross-repository percolation flux, illustrating the effects of a generic thermal-mechanical altered zone (Ofoegbu et al., 2001)

were examined by making the altered zone function as a flow barrier or conduit through a manipulation of the directional permeability. The altered zone was made to function as a barrier by decreasing the aperture of vertical fractures, or conduit by increasing the aperture of horizontal fractures.

The profiles of cross-repository percolation flux from cases that included an altered zone are compared with the basecase (Figure 7). The cross-repository flux for

the basecase is approximately 10 mm/yr., i.e., the same as the input net infiltration flux. Each of the cases that included an altered zone shows a redistribution of cross-repository percolation flux, resulting in a reduced flux at the upstream (up-dip) end and an increased flux at the downstream (down-dip) end of the altered zone (Figure 7). The flux redistribution was caused by lateral diversion of flux within or above the altered zone. The diversion occurred above the altered zone if the zone acted as a flow barrier, or

within the altered zone if the zone acted as a flow conduit. The results in Figure 7 indicate that the cross-repository flux would, in general, be decreased near the up-stream end and increased near the downstream end of a thermal-mechanical altered zone; irrespective of whether the altered zone acts as a flow barrier or conduit.

## 6 CONCLUSIONS

Rock-mass permeabilities near the repository horizon can be expected to increase within laterally discontinuous zones centered at the emplacement drifts and at the middle of the interdrift pillars, owing to fracture dilation associated with thermally induced geomechanical response. The altered zones would be characterized by increased horizontal permeability.

Lateral diversion of moisture within or around the altered zones can be expected and would result in a redistribution of the cross-repository percolation flux.

As a result, cross-repository flux can be expected to be relatively high at the downstream end of the altered zones. Consequently, parts of an emplacement drift close to the downstream end of a thermal-mechanical altered zone can be expected to experience elevated percolation flux.

## ACKNOWLEDGEMENT

This paper was prepared to document work performed by the Center for Nuclear Waste Regulatory Analyses (CNWRA) for the Nuclear Regulatory Commission (NRC) under Contract No. NRC-02-97-009. The activities reported here were performed on behalf of the NRC Office of Nuclear Material Safety and Safeguards, Division of Waste Management. This paper is an independent product of the CNWRA and does not necessarily reflect the view or regulatory position of the NRC. The author thanks B. Dasgupta and B. Sagar for technical reviews of the paper and C. Patton for secretarial support.

## REFERENCES

Barton C.A., M.D. Zoback, & D. Moos. 1995. Fluid flow along potentially active faults in crystalline rock. *Geology* 23: 683-686.

Civilian Radioactive Waste Management System, Management and Operating Contractor. 1999. *License Application Design Selection Report*, B00000000-01717-4600-00123 Rev. 01. Las Vegas, NV: Office of Civilian Radioactive Waste Management.

Civilian Radioactive Waste Management System, Management and Operating Contractor. 2000. *Site Recommendation Subsurface Layout*, ANL-SFS-MG-000001 Rev. 00. Las Vegas, NV: Office of Civilian Radioactive Waste Management.

Hibbitt, Karlsson, & Sorensen, Inc. 1998. *ABAQUS User's Manual: Version 5.8*. Pawtucket, RI: Hibbitt, Karlsson, & Sorensen, Inc.

Lichtner P.C., M.S. Seth, & S. Painter. 2000. *MULTIFLO User's Manual, MULTIFLO Version 1.2: Two-Phase Nonisothermal Coupled Thermal-Hydrological-Chemical Flow Simulator*. San Antonio, TX: Center for Nuclear Waste Regulatory Analyses. Ofoegbu G.I. 1999. Variations of drift stability at the proposed Yucca Mountain repository. In B. Amadei, R.L. Kranz, G.A. Scott, & P.H. Smeallie (eds.), *Rock Mechanics for Industry; Proc. 37th U.S. Rock Mech. Symp.*, Vail, 6-9 June 1999. Rotterdam: Balkema.

Ofoegbu G.I. 2000. *Thermal-Mechanical Effects on Long-Term Hydrological Properties at the Proposed Yucca Mountain Nuclear Waste Repository*, CNWRA 2000-03. San Antonio, TX: Center for Nuclear Waste Regulatory Analyses.

Ofoegbu G.I., S. Painter, R. Chen, R.W. Fedors, & D.A. Ferrill. 2001. Geomechanical and thermal effects on moisture flow at the proposed Yucca Mountain nuclear waste repository. *Nuclear Technology* 127: In press.

Snow D.T. 1968. Rock fracture spacings, openings, and porosities. *Proceedings of the American Society of Civil Engineers; Journal of the Soil Mechanics and Foundations Division* 94(SM1): 73-91.

Wei Z.Q., P. Egger, & F. Descoedres. 1995. Permeability predictions for jointed rock masses. *International Journal of Rock Mechanics and Mining Sciences and Geomechanics Abstracts* 32(3): 251-261.